THROUGH-THE-SONAR SEAFLOOR CHARACTERIZATION USING LACUNARITY

David P. Williams NATO STO CMRE, La Spezia, Italy

1 INTRODUCTION

Increasingly, mine countermeasures (MCM) operations are conducted with an autonomous underwater vehicle (AUV) equipped with side-looking sonars. To enable *adaptive* surveys in which the AUV can automatically adjust to the environmental and tactical conditions observed *in situ*, it is helpful to have an accurate understanding of the seafloor characteristics. This is due to the fact that there exists a strong functional relationship between the characteristics of the seafloor and the relative difficulty of detecting objects (e.g., mines) in side-looking sonar imagery. (The generic umbrella term "characteristics" can refer to *sediment composition*, which affects target to seabed-reverberation levels, as well as *seafloor complexity*, influenced by topography, rocks, and vegetation.) As a result, knowledge of the seafloor conditions can translate into more intelligent surveys, more accurate predictions of detection performance, and more effective automatic target recognition algorithms. In this work, we propose a new, fast approach to characterizing the seafloor in sonar imagery that is particularly well-suited for AUV-based MCM operations.

Because seafloor variation often occurs on a very short length-scale (of meters), a global estimate of the environment (over a site spanning potentially many square kilometers) based on very few discrete measurement points (e.g., sediment grab samples) is typically too coarse to be of value. Instead, there is a need to accurately characterize the seafloor conditions locally, with through-the-sensor sonar data being a logical means.

A common approach to assessing an underwater environment is to perform (hard) segmentation of the seafloor into discrete classes (e.g., sand, mud, rock). Various supervised classification approaches (requiring labeled training data) have been used to achieve this, with methods employing sets of features based on fractal dimension[1], gray-level co-occurrence matrices[2], spectral energy[3], wavelets[4], or combinations thereof[5]. The major problem with these approaches is that the complete universe of seafloor classes must be known and enumerated *a priori*. Thus, there is a desire to instead characterize each point on the seafloor via a single continuous-valued feature, without having to resort to explicit class segmentation.

Some of the earliest attempts to characterize seafloors in sonar imagery were based on trying to fit specific statistical models to the pixel distribution[6,7]. The learned model parameters (e.g., the shape parameter of a *k*-distribution) would then be used to implicitly characterize the seafloor. The main drawback to this approach is that there is no guarantee that the pixels actually follow the assumed distribution. Although the approach may work well on ideal, benign flat seabeds where the parameters are tightly correlated with the sediment (scatterer) size, it is unclear that more complex seafloors – e.g., covered in posidonia (a type of seagrass), characterized by sand ripples, or composed of a mixture of sediments – satisfy the implicit assumptions.

More recently, features quantifying the anisotropy and complexity of sonar images were introduced[8,9] as promising ways to characterize the seafloor. These features measure the variation and average, respectively, of filter responses from a family of two-dimensional Haar-like filters rotated at different angles. Although these features are currently the most appealing solution, their

performance is limited. Among other issues, these features often struggle to distinguish flat seabed from seabed covered by posidonia.

In this work, we instead propose the use of lacunarity, which is a measure of pixel-intensity variation, to characterize seafloors in sonar imagery. Lacunarity has been used successfully for similar environmental assessment purposes in other domains, such as with imagery from synthetic aperture radar (SAR)[10], hyperspectral[11], and lidar[12] sensors. Here we demonstrate that lacunarity can be applied to the underwater domain for environmental characterization, which has not been shown previously. (Previous work exploiting lacunarity with sonar data used the concept only for anomaly detection, namely, to distinguish pure speckle from regions with structure[13] and to detect objects within sand ripples[14,15].)

The remainder of this paper is organized as follows. Section 2 discusses lacunarity and shows how it can be computed quickly. Section 3 provides an overview of the measured sonar data used in the experiments and presents some results. Concluding remarks and directions for future work are given in Section 4.

2 LACUNARITY

Lacunarity was originally developed as a way to measure spatial structure in binary-valued data[16], but the concept has since been extended to quantify pixel-intensity variation in grayscale imagery[17]. In this work, lacunarity is used to characterize the seafloor in sonar imagery.

The lacunarity of a set of pixels in a grayscale image is the ratio of the variance of the pixel values to the square of the mean of the pixel values. When the set corresponds to indices that constitute a rectangular block of pixels, this calculation can be done quickly using integral images.

An integral image[18] is an image representation that allows for very fast computation of rectangular, Haar-like features at any scale or location in constant time (since the computation does not depend on the size of the input). The construct was formulated in the computer-vision field, where it is used extensively for real-time applications.

Starting from an original (sonar) image, **X**, the corresponding integral image, **I**, is constructed as follows. The value at a location *(r,c)* in the integral image corresponds to the sum of the pixels above and to the left of *(r,c)*, inclusive, in the original image, **X**. The integral image is generated using the recursive relation $I(r,c) = I(r-1,c) + z(r,c)$, where $z(r,c)$ is the cumulative sum of pixels in a row of the original image, $z(r,c) = z(r,c-1) + X(r,c)$.

This can be efficiently implemented in Matlab in a single line of code:

```
I = cumsum(cumsum(X,2),1).
```

Next let $\mathbf{X}^p$ indicate the image that results from raising each pixel value to the power p, and let $\mathbf{I}_p$ denote the associated integral image. Computing the lacunarity over the sonar image **X** requires two integral images, $\mathbf{I}_1$ and $\mathbf{I}_2$.

The sum of pixel values in a rectangular area about a given location is computed quickly with only four array accesses of the integral image, as $S_p(r,c) = I_p(r-a,c-b) - I_p(r-a,c+b) - I_p(r+a,c-b) + I_p(r+a,c+b)$, where a and b are the fixed numbers of pixels contained in half of a side (length and width, respectively) of the rectangle. Thus, $\mathbf{S}_p$ can be computed for an entire image at once without resorting to any loops.

After computing $\mathbf{S}_p$ for $p=1,2$, the final lacunarity map (associated with the *entire* sonar image), **L**, can be quickly computed as $\mathbf{L} = (n\mathbf{S}_2 / (\mathbf{S}_1)^2) - \mathbf{1}$, where $n=4ab$ is the number of pixels summed in the rectangle, the exponentiation and division are performed element-wise, and **1** is an appropriately-sized matrix of ones.

In this work, the size of the rectangle used in the lacunarity calculation is 2 m x 2 m (corresponding to *a=40* pixels in the along-track direction and *b=66* pixels in the range direction, respectively, for the high-resolution sonar images). This size is chosen to be large enough to capture distinguishing (textural) characteristics of the seafloor, but small enough to respect the short length-scale at which seafloor conditions are known to vary.

It should also be noted that particular care must be taken to ensure that the precision of the integral-image computations is sufficiently high. If not, errors that can accumulate and grow quickly might manifest[19]. To verify that the precision used is adequate, one can regenerate the original (sonar) image from the integral image via the identity $X(r,c) = I(r-1,c-1) - I(r-1,c) - I(r,c-1) + I(r,c)$ and confirm that no errors have been introduced. In this work, double-precision data types were sufficient.

3 EXPERIMENTAL RESULTS

The feasibility of using lacunarity for seafloor characterization is evaluated in this work using real, measured sonar data collected at sea. The set of data used in this study was collected by the CMRE's SAS-equipped AUV called MUSCLE. The center frequency of the SAS is 300 kHz, and the bandwidth is approximately 60 kHz. The system enables the formation of high-resolution sonar imagery with a theoretical across-track resolution of 1.5 cm and a theoretical along-track resolution of 2.5 cm. A standard SAS image from this system comprises over 14 million pixels. The images considered in the following analysis were drawn from data collected during nine major sea experiments that were conducted by NURC/CMRE between 2008 and 2014 at various geographical sites in the Baltic and Mediterranean Seas.

3.1 Benign Seabed

First we examine the ability of lacunarity to more finely distinguish benign flat seabed. To this end, one example SAS image was selected from each of the nine sea experiments. These nine images, which were selected because they were relatively featureless, are shown in Figure 1.

Although the seabed in all of the images is benign, the sediment composition is expected to be different, since the geographical locations are diverse. (Sediment maps of the experiment locations – i.e., with coarse classes such as mud, sand, gravel – also suggest that the seabed compositions should differ.) The lacunarity centered around each pixel in an image is then computed. The resulting probability density of these lacunarity values is shown in Figure 2 for each of the nine images.

From the figure, it can be observed how the lacunarity values vary slightly among the experiments. For example, the lacunarity values are very low for the COL2 experiment, conducted near Riga in the Baltic Sea, where the seabed was expected to be composed of mud. The other experiments were conducted at various locations in the Mediterranean Sea, where a sandy bottom was expected. The lacunarity values for these cases are higher, yet still differ among experiments. We hypothesize that the larger the grain size, the higher the lacunarity value. Unfortunately, sediment grab samples are not possessed for these specific locations, so a correspondence between lacunarity and grain size cannot be established. However, that study would be of interest if the sediment samples can be obtained in the future.

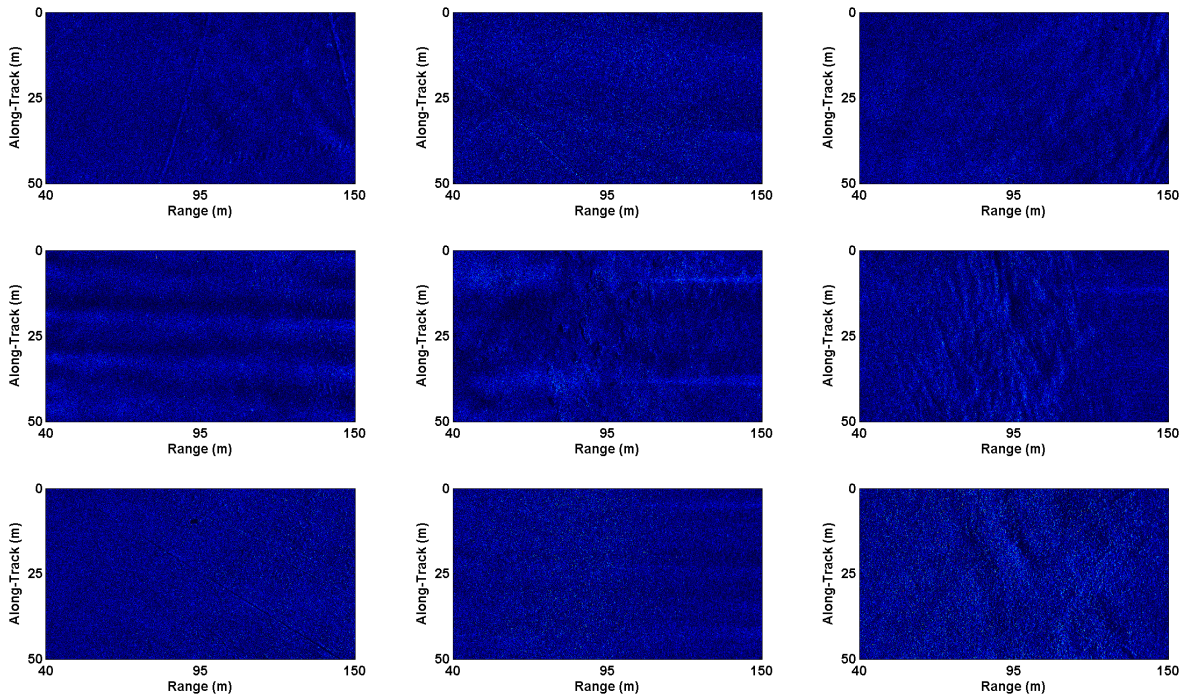

Figure 1: One example SAS image of benign seabed from each of the nine sea experiments (experiment codes, from top left, row-wise: COL2, CAT1, CAT2, AMI1, ARI1, ARI2, SPM1, MAN2, MAN1).

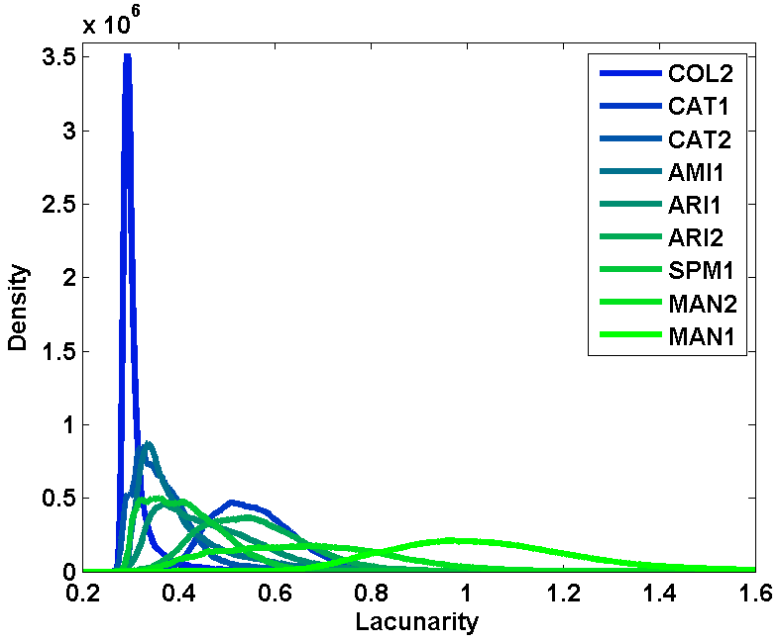

Figure 2: Probability densities of the lacunarity values computed from the SAS images in Figure 1.

3.2 Complex Seabed

Next we examine the ability of lacunarity to distinguish different seabed types in complex scenes. Due to space constraints, results are shown for only two interesting SAS images, though these images allow us to discuss various elements of the lacunarity-based approach. One desired result is to be able to distinguish benign seabed, posidonia, and rocky areas. Another goal is to be able to distinguish benign seabed from ostensibly featureless regions that are actually characterized by poor image quality.

To illustrate the appeal of lacunarity for these tasks, we also calculate other features that could be used in this context. Specifically, we consider the Haar-filter-based complexity and anisotropy features, as well as the simple pixel average (computed over the same sized boxes used for lacunarity).

Figure 3 shows one SAS image with a complex scene, while Figure 4 shows the corresponding feature "maps" of the four features considered – lacunarity, complexity, anisotropy, pixel average. Visual comparison of the SAS image and the feature maps can reveal some of the shortcomings of the competing approaches. For example, complexity has difficulty distinguishing the posidonia in the upper left portion of the image from benign seabed. To effect a hard segmentation of the lacunarity map for the SAS image, a simple set of "class" thresholds is employed: purple, (0,0.3]; blue, (0.3,0.8]; green, (0.8,1.2]; red, [1.2,∞). Roughly speaking, these color classes associate to seabed types as follows: purple corresponds to poor image quality regions and shadows, blue corresponds to benign seabed, green corresponds to posidonia, and red corresponds to rocky complex areas. The hard-segmentation result based on lacunarity for Figure 3 is shown in Figure 5, where it can be observed that the result is quite reasonable in distinguishing seabed types.

A second set of results is shown for another interesting SAS image, shown in Figure 6. The feature maps are shown in Figure 7 and the resulting hard-segmentation based on lacunarity is shown in Figure 8. Again, the segmentation result seems very reasonable. Of particular interest is how the regions of poor image quality at long range were successfully distinguished from benign flat seabed.

A large-scale, objective assessment of the segmentation capability – with thresholds learned using a set of labeled training data – can be conducted in the future on larger data sets. But the present anecdotal evidence suggests that the lacunarity-based approach for characterizing the seabed is indeed promising.

4 CONCLUSION

A new approach for characterizing seafloor in side-looking sonar imagery was proposed. The approach is based on lacunarity, which measures pixel-intensity variation, of through-the-sensor data. This simple yet powerful scalar quantity has the ability to distinguish different seabed types and to identify regions of poor image quality. Moreover, it can be computed very quickly, making real-time seafloor assessments onboard an AUV feasible.

There are several topics that would be worth exploring as future work. If sediment grab samples could be obtained at the locations of the imagery considered, it may be possible to establish a functional relationship between lacunarity and seabed sediment type. Additionally, if manually created ground truth specifying seabed type for a large set of images were created, more principled class thresholds could be learned properly and objective measures of performance could be obtained.

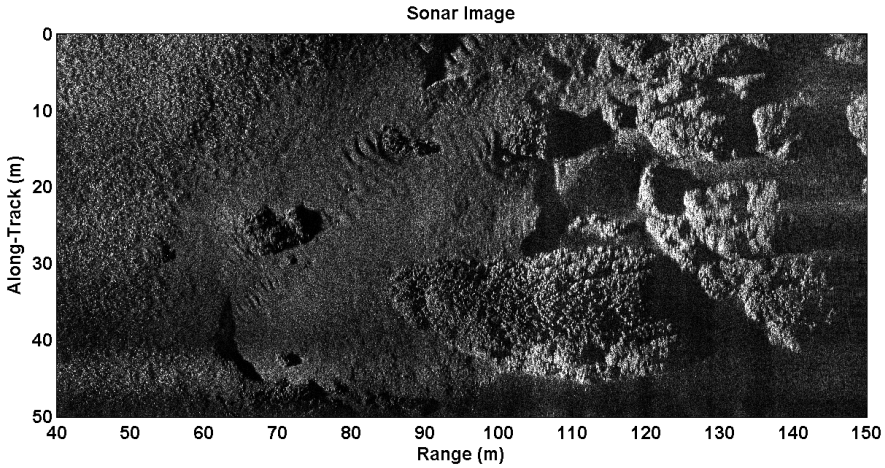

Figure 3: Example SAS image of a complex environment.

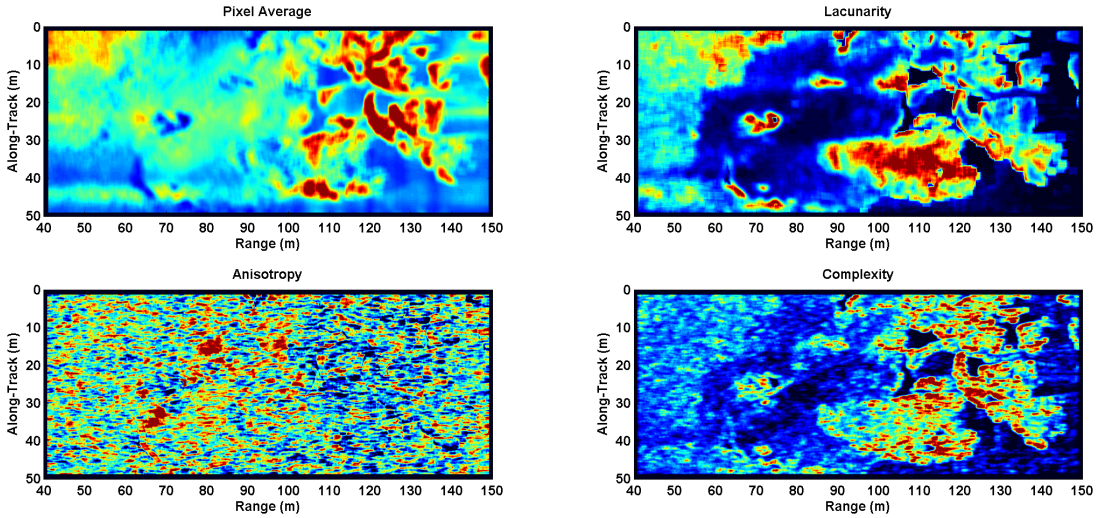

Figure 4: The values of different features for the SAS image in Figure 3, for characterizing the environment. The features, clockwise from top-left are: pixel average, lacunarity, complexity, and anisotropy.

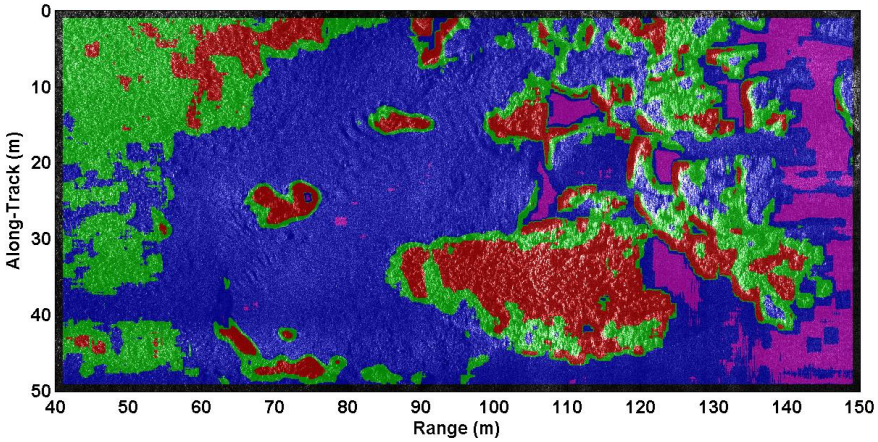

Figure 5: Example hard-segmentation result of the SAS image in Figure 3 based on the lacunarity values, where purple corresponds to poor image quality regions and shadows, blue corresponds to benign seabed, green corresponds to posidonia, and red corresponds to rocky complex areas.

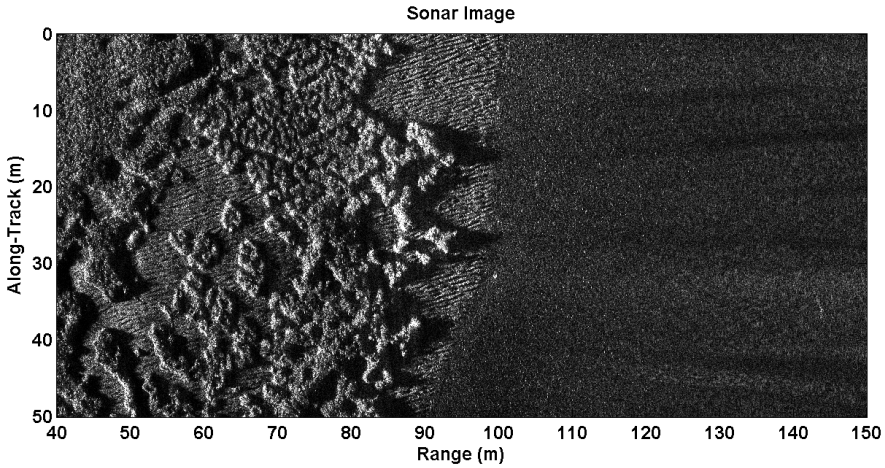

Figure 6: Example SAS image of a complex environment.

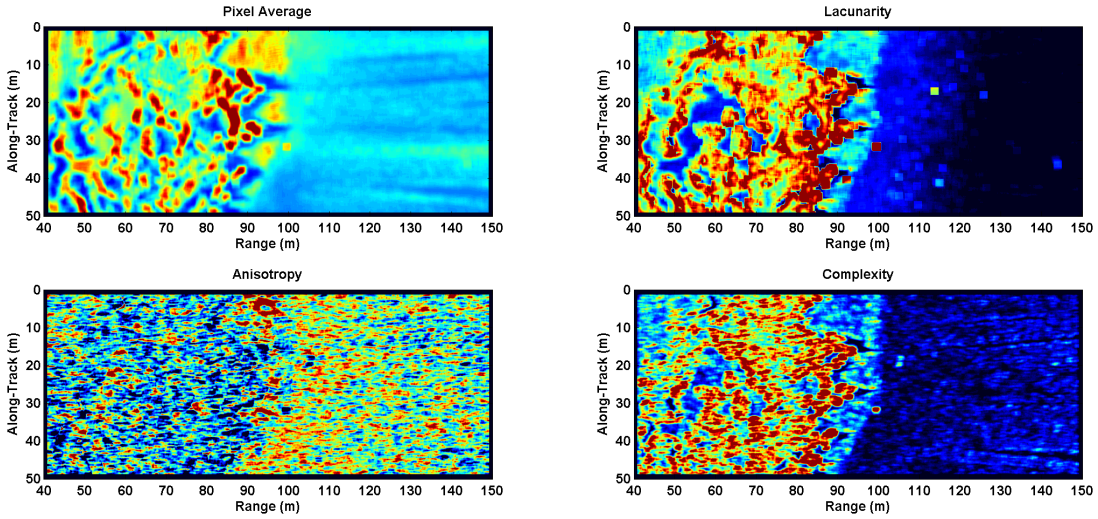

Figure 7: The values of different features for the SAS image in Figure 6, for characterizing the environment. The features, clockwise from top-left are: pixel average, lacunarity, complexity, and anisotropy.

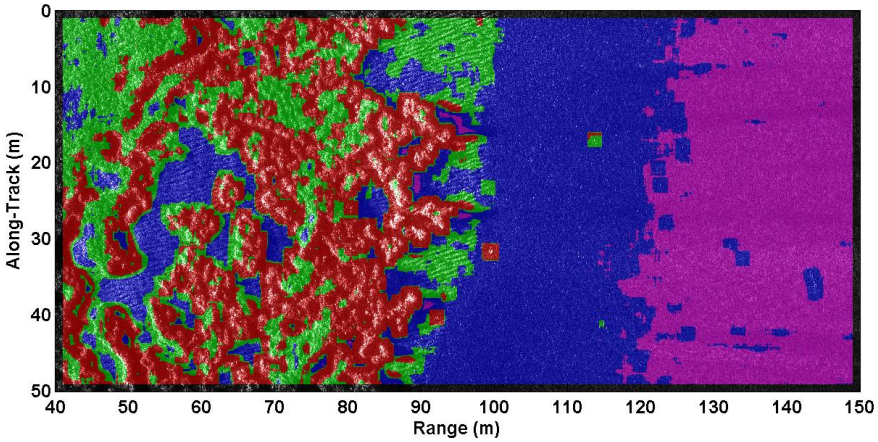

Figure 8: Example hard-segmentation result of the SAS image in Figure 6 based on the lacunarity values, where purple corresponds to poor image quality regions, blue corresponds to benign seabed, green corresponds to posidonia and sand ripples, and red corresponds to rocky complex areas.

5 REFERENCES

1. D. Carmichael, L. Linnett, S. Clarke, and B. Calder, “Seabed classification through multifractal analysis of sidescan sonar imagery,” *IEE Radar, Sonar and Navigation*, vol. 143, no. 3, pp. 140–148, 1996.
2. P. Blondel, L. Parson, and V. Robigou, “TexAn: Textural analysis of sidescan sonar imagery and generic seafloor characterisation,” in *Proc. IEEE OCEANS*, vol. 1, 1998, pp. 419–423.
3. S. Reed, I. Ruiz, C. Capus, and Y. Petillot, “The fusion of large scale classified sidescan sonar image mosaics,” *IEEE Transactions on Image Processing*, vol. 15, no. 7, pp. 2049–2060, 2006.
4. D. Williams, “Bayesian data fusion of multiview synthetic aperture sonar imagery for seabed classification,” *IEEE Transactions on Image Processing*, vol. 18, no. 6, pp. 1239–1254, 2009.
5. I. Karoui, R. Fablet, J. Boucher, and J. Augustin, “Seabed segmentation using optimized statistics of sonar textures,” *IEEE Transactions on Geoscience and Remote Sensing*, vol. 47, no. 6, pp. 1621–1631, 2009.
6. D. Abraham and A. Lyons, “Novel physical interpretations of K-distributed reverberation,” *IEEE Journal of Oceanic Engineering*, vol. 27, no. 4, pp. 800–813, 2002.
7. D. Abraham and A. Lyons, “Reliable methods for estimating K-distribution shape parameter,” *IEEE Journal of Oceanic Engineering*, vol. 35, no. 2, pp. 288–302, 2010.
8. O. Daniell, Y. Petillot, and S. Reed, “Unsupervised sea-floor classification for automatic target recognition,” in *Proc. International Conference on Underwater Remote Sensing*, 2012.
9. E. Fakiris, D. Williams, M. Couillard, and W. Fox, “Sea-floor acoustic anisotropy and complexity assessment towards prediction of ATR performance,” in *Proc. International Conference and Exhibition Underwater Acoustics*, 2013, pp. 1277–1284.
10. G. Henebry and H. Kux, “Lacunarity as a texture measure for SAR imagery,” *Remote Sensing*, vol. 16, no. 3, pp. 565–571, 1995.
11. S. Myint, C. Giri, L. Wang, Z. Zhu, and S. Gillette, “Identifying mangrove species and their surrounding land use and land cover classes using an object-oriented approach with a lacunarity spatial measure,” *GIScience & Remote Sensing*, vol. 45, no. 2, pp. 188–208, 2008.
12. J. Weishampel, J. Blair, R. K. R. Dubayah, and D. Clark, “Volumetric lidar return patterns from an old-growth tropical rainforest canopy,” *International Journal of Remote Sensing*, vol. 21, no. 2, pp. 409–415, 2000.
13. R. Kessel, “Using sonar speckle to identify regions of interest and for mine detection,” *AeroSense 2002*, pp. 440–451, 2002.
14. J. Nelson and N. Kingsbury, “Fractal dimension, wavelet shrinkage and anomaly detection for mine hunting,” *IET Signal Processing*, vol. 6, no. 5, pp. 484–493, 2012.
15. J. Nelson and V. Krylov, “Textural lacunarity for semi-supervised detection in sonar imagery,” *IET Radar, Sonar & Navigation*, vol. 8, no. 6, pp. 616–621, 2014.
16. B. Mandelbrot, *The Fractal Geometry of Nature*. Macmillan, 1983, vol. 173.
17. R. Plotnick, R. Gardner, W. Hargrove, K. Prestegaard, and M. Perlmutter, “Lacunarity analysis: A general technique for the analysis of spatial patterns,” *Physical Review E*, vol. 53, no. 5, pp. 5461–5468, 1996.
18. P. Viola and M. Jones, “Robust real-time object detection,” *International Journal of Computer Vision*, vol. 57, no. 2, pp. 137–154, 2004.
19. G. Facciolo, N. Limare, and E. Meinhardt, “Integral images for block matching,” *Image Processing On Line*, vol. 4, pp. 344–369, 2014.